MedChemComm

RSC Publishing

CONCISE ARTICLE

Synthesis, structure–activity relationships and stereochemical investigations of new tricyclic pyridazinone derivatives as potential STAT3 inhibitors†

Cite this: *Med. Chem. Commun.*, 2013, **4**, 1181

Daniela Masciocchi,[a] Arianna Gelain,[a] Federica Porta,[a] Fiorella Meneghetti,[a] Alessandro Pedretti,[a] Giuseppe Celentano,[a] Daniela Barlocco,[a] Laura Legnani,[be] Lucio Toma,[b] Byoung-Mog Kwon,[c] Akira Asai[d] and Stefania Villa*[a]

Received 27th March 2013
Accepted 19th June 2013

DOI: 10.1039/c3md00095h

www.rsc.org/medchemcomm

Through a cell-based biological screening, the benzocinnolinone derivative (±)-**2c** was identified as a promising STAT3 inhibitor. Since SAR studies on a series of compounds structurally related to (±)-**2c** (**1c**, **2a–p**, **3c**, **4c**, **6**) showed that the latter had the most significant inhibitory activity, we investigated in depth its essential structural features. In particular, enantiomeric separation was performed, and the absolute configuration of the stereoisomers was assigned by theoretical and crystallographic studies. The biological evaluation highlighted that (*S*)-(−)-**2c** is twice as potent as (*R*)-(+)-**2c**.

Introduction

Signal Transducer and Activator of Transcription 3 (STAT3) is a member of STAT family that comprises seven isoforms (STAT1-4, 5a, 5b, 6). They directly relay signals from the cytoplasmic membrane to the nucleus[1] and regulate transcription of target genes. STAT activation is triggered by many cytokines and growth factors including epidermal growth factor (EGFR), platelet-derived growth factor (PDGF), IL-6, as well as oncogenic proteins such as Src and Ras and, in addition, several carcinogens (*e.g.* cigarette smoke, diesel exhaust).[2] Numerous published reports have shown that blocking constitutively activated STAT3 signaling leads to apoptosis of tumor cells,[3–5] but has only minimal effects on normal cells.[6,7] This selective inhibition might reflect an irreversible dependence of tumor cells on the high level of STAT3 for growth and survival, whereas normal cells might be able to withstand lower level STAT3 activity or use alternative signaling pathways. Therefore, the design of new molecules as STAT3 inhibitors, their synthesis and the studies of their interaction with the target are very important for the development of new anticancer drugs endowed with interesting pharmacodynamic properties and reduced side effects.[8]

There are two different approaches to inhibit STAT3 signaling: direct (by the interaction of the compounds with the protein) or indirect (by blocking the upstream molecules). The direct inhibitors can be divided into several classes, *e.g.* peptides, peptidomimetics, natural compounds, small molecules and oligonucleotides, while the indirect ones can be classified as either natural or synthetic compounds.[8] A few representative STAT3 inhibitors, endowed with high activity, are reported in Chart 1. STA21 (**I**, the first non-peptide inhibitor) and CDDO-Me (**II**, a synthetic triterpenoid derivative) are both in clinical trials;[9] the orally bioavailable derivative of STX-0119 (**III**, a quinoline analogue tested *in vivo*)[10] and compound HJC0123 (**IV**)[11] were recently reported while the natural compound Cryptotanshinone (**V**), isolated from *Salvia miltiorrhiza*, initially utilized for the treatment of circulatory disorders was later investigated for STAT3 inhibition.[12] During our ongoing research,[13,14] aimed at the design and synthesis of new non-peptide small molecules as potential STAT3 inhibitors, we screened our internal library using the dual luciferase assay in HCT-116 cells; compound **2c** [ethyl 4-(3-oxo-4,4*a*,5,6-tetrahydrobenzo [*h*] cinnolin-2(3*H*)-yl)butanoate] (Chart 2) showed interesting inhibitory activity (46% at 2 μM).

Given the apparent similarity between our tricyclic hit and Cryptotanshinone, an introductory conformational study was done on the two compounds. Particular attention was focused on the flexibility of the natural compound and on the possible inversion of the central ring of **2c**. Preliminary results seemed to indicate that both structures are quite rigid and characterized

[a]*Dipartimento di Scienze Farmaceutiche, Università degli Studi di Milano, Via Mangiagalli 25, 20133 Milano, Italy. E-mail: stefania.villa@unimi.it; Fax: +39-02-503-19359*

[b]*Dipartimento di Chimica, Università degli Studi di Pavia, Via Taramelli 12, 27100 Pavia, Italy*

[c]*Korea Research Institute of Bioscience & Biotechnology, University of Science and Technology, Eoun-Dong, Yuseong-gu, Daejeon 305-806, Republic of Korea*

[d]*Center for Drug Discovery, Graduate School of Pharmaceutical Sciences, University of Shizuoka, 52-1 Yada, Suruga-ku, Shizuoka, 422-8526, Japan*

[e]*Università degli Studi di Milano, Dipartimento di Biotecnologie Mediche e Medicina Traslazionale, Via Vanvitelli 32, 20133 Milano, Italy*

† Electronic supplementary information (ESI) available. See Electronic supplementary information (ESI) available. CCDC 906024. For ESI and crystallographic data in CIF or other electronic format see DOI: 10.1039/c3md00095h

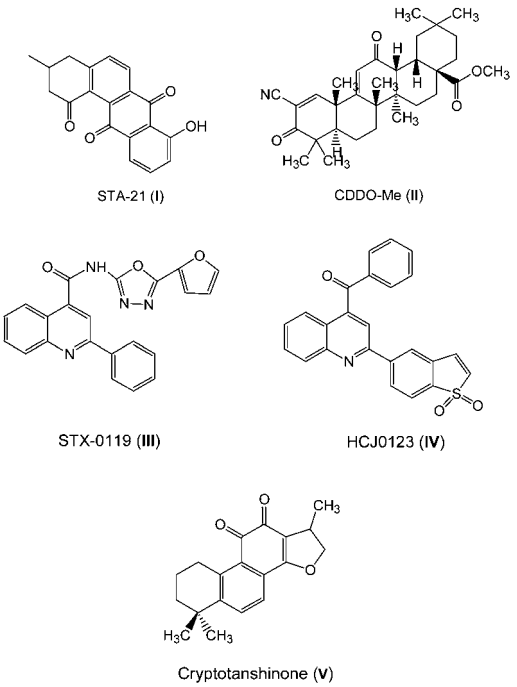

Chart 1

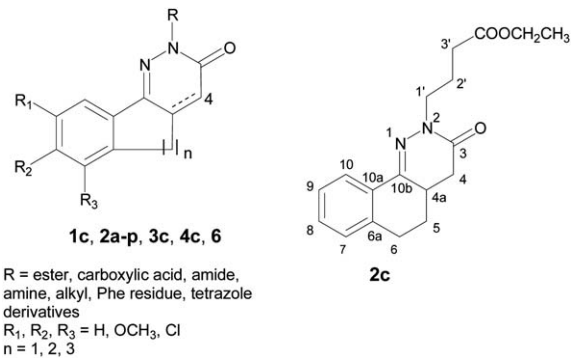

Chart 2

by planarity, an important requisite for the inhibitory activity *versus* STAT3 (unpublished results).

On this basis, since preliminary modifications on **2c**, *e.g.* homologation to the corresponding indenopyridazinone **1c** and benzocycloheptapyridazinone **3c** as well as introduction of a 4–4a double bond (**4c**) proved to be detrimental, the following SAR studies were performed on this hit. In particular, chains of different nature and length (**2a,b,f–p**) as well as substitution of the phenyl ring (**2d,e**) were investigated. All the synthesized compounds were tested by the cell-based dual luciferase assay, at the concentration of 2 μM, in order to determine their ability to lower STAT3 activity. Subsequently, we separated the enantiomers of **2c** to investigate the influence of the stereocenter on its biological activity. In parallel, modeling studies were performed to explore the conformational properties of this class and to understand how the molecular features influenced the $[\alpha]_D$ value, taking into account the experimental $[\alpha]_D$ of the single enantiomers. This allowed the theoretical assignment of the configuration of the stereocenter of **2c**. The absolute configuration was then confirmed by means of crystallographic analysis on the suitable derivative (+)-**13**, containing a chlorine atom. Compound **13** is related to **2c** since both are synthesized *via* N-2 alkylation of **6**, which occurs with retention of configuration. In summary, we obtained (+)-**13** from (+)-**6**, and (−)-**2c** from (−)-**6**.

Chemistry

The synthesis of the ester derivatives **1c**, **2a–h** and **3c**, characterized by five, six and seven-carbon atom central rings respectively, was performed through alkylation at the N-2 position of the required pyridazinone,[15,16] with suitable bromo ester chains, as shown in Scheme 1. **2b** and **2c** were easily hydrolyzed into the corresponding acids **2i** and **2j** and **2j** was subsequently converted to the ethyl amide **2k**. The amino derivative **2l** was prepared from **6** by alkylation of 1,4-dibromobutane under microwave irradiation followed by condensation with ethylamine. The alkyl derivatives **2m** and **2n** were obtained through alkylation of **6** with the required bromo derivative. Compound **2o** was synthesized by alkylation of **6** with 1-chloropropanol to give intermediate **10**, which was firstly coupled with N-Boc-Phe-OH and then deprotected to form **2o**. For the synthesis of the derivative **2p**, benzocinnolinone **6** was alkylated with 4-bromobutyronitrile and the so obtained nitrile **12** was converted to the tetrazole **2p**. During the synthesis of **4c**, compound **6** was firstly oxidized to 5,6-dihydrobenzo[*h*]cinnolin-3(2*H*)-one **8**, following a previously described procedure[15] and subsequently alkylated with ethyl 4-bromobutanoate. Finally, the enantiomeric separation was performed on (±)-**2c** using a chiral semi-preparative HPLC (Chiralcel OJ, 10 μm, 250 × 4.6 mm); the two stereoisomers were obtained as oils with ee > 99% and were characterized by $[\alpha]_D$ values of +374 and −365. In parallel, the enantiomeric separation of the intermediate (±)-**6** was performed using the same conditions, obtaining two enantiomers characterized by $[\alpha]_D$ values of +572 and −561, respectively. Enantiomer (−)-**6** was alkylated with ethyl 4-bromo-butanoate under microwave irradiation to give (−)-**2c** (see the Experimental part). Following the same procedure, by treatment of (+)-**6** with 2-bromo-1-chloroetane, compound (+)-**13** was obtained (Scheme 1).

Results and discussion

Compounds **1c**, **2a–p**, **3c**, **4c**, and **6** were tested by a dual-luciferase assay[17] at a concentration of 2 μM in HCT-116 cells after 24 h of treatment. Their activities were compared to that of the natural compound Cryptotanshinone and the results are reported in Table 1. As can be seen, each modification on **2c**, namely elimination (**6**), shortening (**2b**) or elongation (**2f**) of the ester chain, as well as its substitution with alkyl moieties (**2m**) caused a decrease in the activity. Similarly, hydrolysis of the ester group (**2j**) or its substitution by different functionalities (**2k,l,o,p**) had a detrimental effect. These results highlight the importance of the chain at the N-2 position and of its nature. Also the presence of different substituents on the phenyl ring (**2d,e**) did not prove to be beneficial.

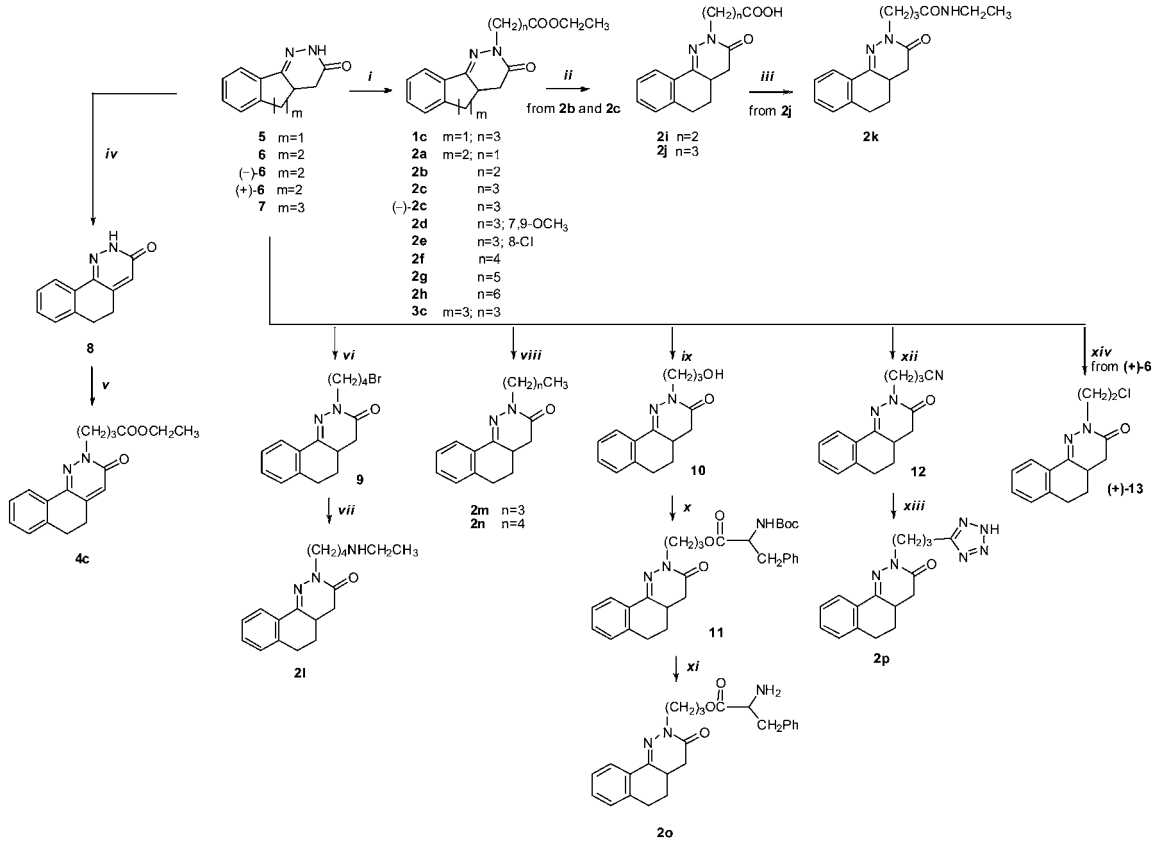

Scheme 1 *Reagents and conditions*: (i) $Br(CH_2)_nCOOCH_2CH_3$, NaH, dry DMF, 70 °C, 15 h; (ii) NaOH/H_2O, EtOH, reflux, 2 h; (iii) $EtNH_2$ 70% in water, HATU, *N*-methyl-morpholine, rt, 1.5 h; (iv) *m*-nitrobenzensulfonic acid sodium salt, NaOH, H_2O, reflux, 0.5 h; (v) $Br(CH_2)_3COOCH_2CH_3$, KOH, TBAF, toluene, 50 °C; (vi) $Br(CH_2)_4Br$, NaH, dry DMF, MW 60 °C, 10 min; (vii) 70% $EtNH_2$ in water, Et_3N, DMF, 90–100 °C, 7 h; (viii) $Br(CH_2)_nCH_3$, NaH, dry DMF, 70 °C, 10 h; (ix) $Cl(CH_2)_3OH$, NaH, dry DMF, 60 °C, 4 h; (x) N-Boc-Phe-OH, HATU, *N*-methyl-morpholine, rt, 24 h; (xi) trifluoroacetic acid, CH_2Cl_2, rt, 3 h; (xii) $Br(CH_2)_3CN$, dry DMF, NaH, 50 °C, 3 h; (xiii) NaN_3, $ZnBr_2$ isopropanol/H_2O 1 : 2, MW 170 °C, 1 h; (xiv) $Br(CH_2)_2Cl$, NaH, dry DMF, MW 70 °C, 15 min.

It should be noted that the alpha-screen based assay[18] did not show any significant interaction between **2c** and the STAT3 SH2 domain, therefore **2c** should be considered as an indirect inhibitor.

When the enantiomers of **2c** were investigated by the luciferase assay at 10 μM concentration, (−)-**2c** resulted to be about two-fold more potent than (+)-**2c**, as shown in Fig. 1.

As the two stereoisomers of **2c** (Chart 2) were obtained as oils, their absolute configurations were initially assigned through theoretical calculations. Preliminary modeling studies were carried out, as the complete knowledge of the allowed conformations of **2c** is a necessary pre-requisite for the optical rotation theoretical prediction. All the calculations were carried out at the B3LYP/6-311+G(d,p) level. The tricyclic moiety was shown to assume a geometry in complete agreement with that described in a previous paper and obtained with a molecular mechanics approach.[19] The main degree of conformational freedom is represented by the N2 side chain that was shown to be able to assume two almost isoenergetic orientations, characterized by values of τ_1(N1–N2–C1′–C2′) of −84° and 78° to give conformers **A** and **B**, respectively (Fig. 2).

Starting from the located conformations, the specific optical rotation of stereoisomer (*R*)-**2c** was predicted using DFT calculations at the same level as above.[20] The calculated $[\alpha]_D$ of the two conformations **A** and **B** of (*R*)-**2c** were +419 and +682, respectively, in reasonable agreement with the experimental value, allowing to assign the *R* configuration to (+)-**2c**. Because of the high value of the specific rotation and the large influence of the N2 side chain on it, we performed new DFT calculations in order to evaluate the contribution of the molecular substructures. In summary, we investigated: (i) the intrinsic properties of the pyridazinone system exemplified by **14** (Fig. 3) and (ii) the effect of the presence and orientation of a phenyl group linked to the pyridazinone as in compound **15** (Fig. 3). Compound **14** shows a value of $[\alpha]_D = +292$, while **15**, characterized by the almost planar arrangement of the two rings (τ_2(C10–C10a–C10b–N1) = −14°), exhibits an optical rotatory power significantly increased ($[\alpha]_D = +731$).

In addition, with the aim of identifying the relationship between the mutual orientation of the two rings and $[\alpha]_D$, we determined the energy profile for rotation around the C–C bond linking the two rings, calculating $[\alpha]_D$ for every step of the scan (the resulting profile is reported in Fig. S1 of the ESI†). In the nearly planar molecular arrangements, characterized by $\tau_2 = 0°$, −30°, +150°, and −180°, $[\alpha]_D$ presents high values, *i.e.* +679, +764, +719, and +701, respectively. By contrast, the perpendicular arrangement of the phenyl and pyridazinone rings causes a lowering of $[\alpha]_D$, that is +238 for $\tau_2 = -90°$ and +221 for $\tau_2 = 90°$.

Table 1 Physico-chemical and biological data for compounds **1–4**, and **6**

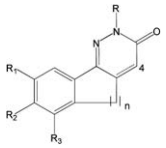

Compound	R	R_1=R_3	R_2	*n*	C at position 4	Eluent[a]	Yield (%)	Mp (°C)	Inhibitory activity[b] (%)
Cryptotanshinone									25
1c	$(CH_2)_3COOEt$	H	H	1	CH_2	B	55	Oil	28
2a	$(CH_2)COOEt$	H	H	2	CH_2	C	71	Oil	3
2b	$(CH_2)_2COOEt$	H	H	2	CH_2	B	61	Oil	30
2c	$(CH_2)_3COOEt$	H	H	2	CH_2	A	60	Oil	46
2d	$(CH_2)_3COOEt$	OCH_3	H	2	CH_2	B	56	96–97	23
2e	$(CH_2)_3COOEt$	H	Cl	2	CH_2	C	60	45	9
2f	$(CH_2)_4COOEt$	H	H	2	CH_2	C	65	Oil	21
2g	$(CH_2)_5COOEt$	H	H	2	CH_2	B	70	Oil	25
2h	$(CH_2)_6COOEt$	H	H	2	CH_2	B	70	Oil	22
2i	$(CH_2)_2COOH$	H	H	2	CH_2	A	97	195–196	−2
2j	$(CH_2)_3COOH$	H	H	2	CH_2	A	95	166–166	8
2k	$(CH_2)_3CONHEt$	H	H	2	CH_2	A	83	136–137	16
2l	$(CH_2)_4NHEt$	H	H	2	CH_2	A	50	Oil	3
2m	$(CH_2)_3CH_3$	H	H	2	CH_2	D	75	Oil	−9
2n	$(CH_2)_4CH_3$	H	H	2	CH_2	D	80	Oil	22
2o	(CH_2)OPhe	H	H	2	CH_2	B	50	Oil	−12
2p	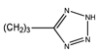	H	H	2	CH_2	A	46	Oil	−9
3c	$(CH_2)_3COOEt$	H	H	3	CH_2	C	40	Oil	−12
4c	$(CH_2)_3COOEt$	H	H	2	CH	B	98	Oil	1
6	H	H	H	2	CH_2	—	—	Oil	−6

[a] Eluent: (A) dichloromethane/methanol 95 : 5; (B) dichloromethane/ethyl acetate 6 : 4; (C) petroleum ether/ethyl acetate 7 : 3; (D) petroleum ether/ethyl acetate 9 : 1. [b] The inhibitory activity of the compounds against STAT3 was evaluated using the dual-luciferase assay in HCT-116 cells at a concentration of 2 μM after 24 h of treatment. The values of STAT3 inhibitory activity were the means of 3 experiments and the maximum deviation from the mean was less than 10%.

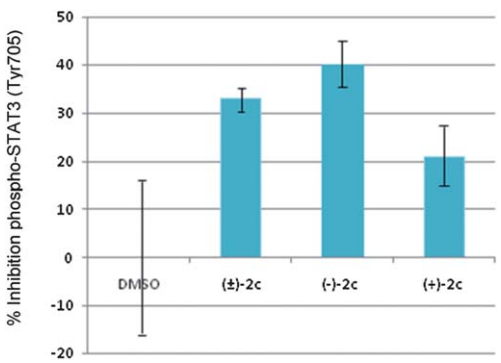

Fig. 1 Dual-luciferase assay results of compounds (±)-**2c**, (−)-**2c**, and (+)-**2c**. The test was carried out in the HCT116 cell line after 24 h treatment with the selected compound (10 μmol L^{-1}).

These results suggest that higher values of $[\alpha]_D$ are related to a greater conjugation of the system.

To give support to the theoretical predictions, the absolute configuration of (+)-**2c** was confirmed by means of crystallographic analysis on the suitable derivative (+)-**13**. We selected

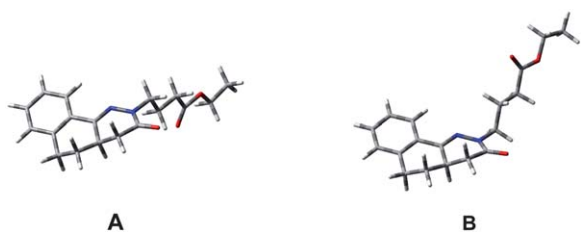

Fig. 2 Three-dimensional plots of conformations **A** and **B** of compound **2c**.

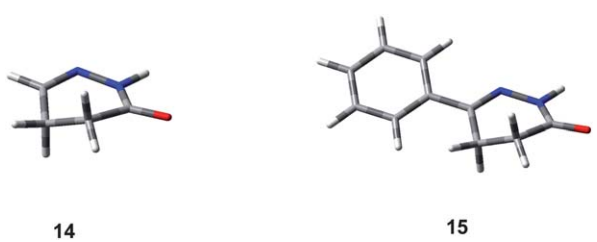

Fig. 3 Three-dimensional plots of compounds **14** and **15**.

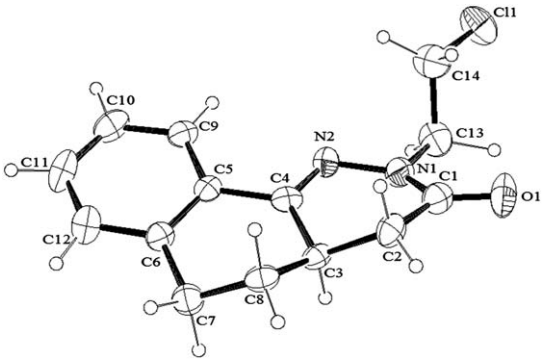

Fig. 4 ORTEP[17] view of the asymmetric unit of (+)-**13** and the relative atom-numbering scheme (thermal ellipsoids at 50% probability).

the ethylenic chain to introduce the chlorine atom on (+)-**6**, as the quality of the crystals for derivatives of this family tended to worsen with longer chains (data not published). Therefore, we considered the ethylenic chain as the compromise for balancing the contrast between the rigid core and the lateral flexible chain. In fact, well diffracting crystals of compound (+)-**13** were obtained, which allowed its crystal structure determination. The ORTEP[21] view of (+)-**13** is shown in Fig. 4.

The chlorine atom gives a significant anomalous dispersion contribution to λ MoKα permitting the unambiguous attribution of the absolute configuration *R* to the enantiomer (+)-**13**. The tricyclic skeleton of the compound consists of three fused rings slightly twisted with respect to each other. The dihedral angles between their least-square planes α (C1/N1/N2/C4/C3/C2), β (C3/C4/C5/C6/C7/C8) and γ (C5/C6/C12/C11/C10/C9) are α–β = 7.0(1)°, α–γ = 16.3(1)°, β–γ = 10.0(1)°, respectively (the arbitrary atom-numbering scheme used in Fig. 4). Therefore, the dihydropyridazinone ring adopts an intermediate geometry between a twisted-boat and a half-chair conformation quantitatively defined by the Cremer & Pople parameters[22] Q_T = 0.430(5) Å, $\phi = -80.0(8)°$, and $\theta = 109.0(6)°$, while the central six-membered ring is almost in a half-boat conformation, characterized by the puckering parameters $Q_T = 0.504(6)$ Å, $\phi = -67.4(7)°$ and $\theta = 58.0(5)°$, with the flap atom C8 out of the best mean plane calculated over the other five carbons by 0.672(6) Å. The orientation of the lateral chain is defined by the torsion angle N2–N1–C13–C14 of 68.7(1)° that corresponds to the value found in the **B** conformer of (*R*)-**2c** resulting from the modeling studies, even though the latter has a much longer side chain.

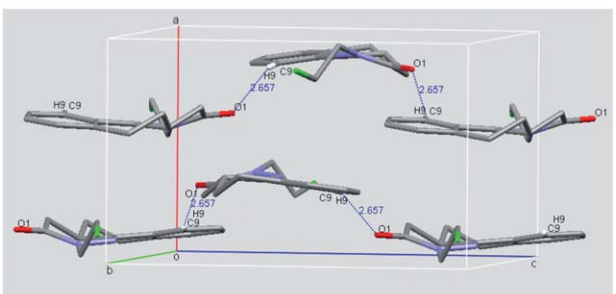

Fig. 5 Intermolecular interactions of (+)-**13**.

In the crystal, the molecules are flattened almost parallel to the plane containing the *b* and *c* axes and are connected through weak Cπ–H$\cdots$O contacts between C9–H9$\cdots$O1^{I} at a distance of 2.66(3) Å and angle of 148(1)° (^{I} at $3/2 - x$, $1 - y$, $z - 1/2$) (Fig. 5).

Finally, in light of the unambiguous assignment of the absolute configuration to (+)-**13** and hence to the **2c** stereoisomers, the enantiomer (*S*)-(−)-**2c** was found to be twice as potent as(*R*)-(+)-**2c** in the luciferase assay.

Conclusion

In an attempt to identify new small molecules as potential STAT3 inhibitors, we screened our internal library using a dual luciferase assay, and found promising activity for the benzocinnolinone derivative **2c**. Since SAR studies on a series of related pyridazinones did not show any improvement in the activity, we focused our attention on the stereocenter of **2c**. In summary, we resolved (±)-**2c** into its enantiomers, which were tested by the luciferase assay in comparison with the racemate. Compound (−)-**2c** resulted to be about two-fold more potent than (+)-**2c**. In order to assign the absolute configuration to the enantiomers, their optical rotatory power was estimated through calculations that allowed us to theoretically assign the *R* configuration to (+)-**2c**. This result was then experimentally confirmed through X-ray analysis on the enantiomerically pure derivative (+)-**13**, structurally related to (+)-**2c**. The crystallographic study unambiguously attributes the *R* configuration to the dextrorotatory enantiomer. On this basis, we could conclude that (*S*)-(−)-**2c** is endowed with better inhibitory activity in the luciferase assay.

Experimental section

Materials and methods

Reagents were purchased from Sigma-Aldrich and were used without any further purification. All reactions involving air-sensitive reagents were performed under a nitrogen atmosphere. The reaction was carried out either under conventional conditions or by means of a Biotage-Initiator microwave synthesizer. Melting points were determined in open capillary tubes on a Büchi Melting Point B-540. Proton NMR spectra were acquired at ambient temperature on a Varian 300 MHz Oxford instrument. Chemical shifts are expressed in ppm from tetramethylsilane resonance in the indicated solvent (TMS: 0.0 ppm). ^{1}H NMR data are reported in the following order: ppm, multiplicity (s, singlet; d, doublet; t, triplet; q, quartet; m, multiplet; br, broad), and number of protons (see ESI†). The course of the reaction was monitored by thin layer chromatography (TLC) on aluminum-backed Silica Gel 60 plates (0.2 mm, Merck). Intermediates and final compounds were purified by flash chromatography using Merck Silica Gel 60 (70–230 mesh). The purity of final compounds was determined by HPLC analysis and was ≥95%. The enantiomeric separation of compounds was performed using a chiral semi-preparative HPLC: Chiralcel OJ (10 μm, 250 × 4.6 mm). Optical rotation values of the enantiomers were registered on a Perkin Elmer instrument (Mod 343) at 589 nm and 25 °C.

General procedure A for the synthesis of the alkylated derivatives (1c, 2a–h, 2m,n, 3c, 10, 12). A solution of the

required pyridazinone derivative (**5–7**) (0.25 mmol) in dry DMF (2 mL) was added to a suspension of sodium hydride (7.2×10^{-3} g, 0.3 mmol) in dry DMF at 0 °C under an inert atmosphere. After 30 min, the appropriate bromo alkyl chain (0.3 mmol) was added and the mixture was stirred for 15 h at 70 °C. Water was cautiously added dropwise to the cooled reaction mixture to destroy the excess of sodium hydride. The mixture was then extracted with ethyl acetate (3×2 mL) and the organic layers were collected, dried over Na_2SO_4, and evaporated *in vacuo*. Upon purification by flash chromatography the final products were obtained. (see Table 1 for data) The enantiomeric separation of compound (±)-**2c** was performed using a chiral semi-preparative HPLC: Chiralcel OJ (10 μm, 250 × 4.6 mm), hexane/ethanol (70 : 30), 1.0 mL min^{-1}, UV 254 nm; $t_R(\mathbf{1}) =$ 1.999 min (49.9%) $[\alpha]_D^{25}$ −364.6 (*c* 0.0082, EtOH); $t_R(\mathbf{2}) = 3.904$ min (50.1%) $[\alpha]_D^{25}$ + 374.4 (*c* 0.0082, EtOH).

General procedure B for the synthesis of 4-(3-oxo-4,4*a*,5,6-tetrahydrobenzo [*h*] cinnolin-2(3*H*)-yl)carboxylic acids 2i,j. The required ester (0.46 mmol) was dissolved in ethanol (5 mL) and an aqueous solution of 1 N NaOH (1 mL) was added. The solution was stirred at reflux for 2 h, then the ethanol was removed under reduced pressure and the residue was diluted with water (5 mL) and extracted with ethyl acetate (1×2 mL). The aqueous layer was acidified with 6 N HCl (1 mL) and extracted with ethyl acetate (3×2 mL). The organic layer was dried over anhydrous Na_2SO_4, filtered and evaporated under reduced pressure. The crude product was purified by flash chromatography (see Scheme 1 and Table 1).

Synthesis of *N*-ethyl-4-(3-oxo-4,4a,5,6 tetrahydrobenzo [*h*] cinnolin-2(3*H*)-yl)-butanamide 2k. To a solution of compound **2j** (3.7×10^{-2} g, 0.13 mmol) in dichloromethane (3 mL), the coupling agent HATU (7.41×10^{-2} g, 0.20 mmol), ethylamine (0.02 mL, 0.35 mmol) and *N*-methyl morpholine (until pH = 7) were added. The mixture was stirred at room temperature for 1 h and then washed with 1 N HCl (2×1 mL), saturated $NaHCO_3$ solution (2×1 mL) and finally with brine (2×1 mL). The organic layer was separated, dried over anhydrous Na_2SO_4 and evaporated *in vacuo.* Purification by flash chromatography afforded the final compound **2k** (see Scheme 1 and Table 1).

2-(4-(Ethylamino)butyl)-4,4*a*,5,6-tetrahydrobenzo[*h*]cinnolin-3(2*H*)-one 2l. To a solution of **6** (5×10^{-2} g, 0.25 mmol) in dry DMF under a nitrogen atmosphere, NaH (7.2×10^{-3} g, 0.3 mmol) and $Br(CH_2)_4Br$ (0.036 mL, 0.3 mmol) were added. The mixture was irradiated for 10 min at 60 °C in a microwave synthesizer. The solvent was evaporated under reduced pressure and the residue was extracted with ethyl acetate (3×2 mL). The organic layer was separated, dried over anhydrous Na_2SO_4, and evaporated *in vacuo*. Upon purification by flash chromatography (eluent: petroleum ether/ethyl acetate 7 : 3) 2-(4-bromobutyl)-4,4*a*,5,6-tetrahydrobenzo[*h*]cinnolin-3(2*H*)-one (**9**) was obtained as a white solid. To a solution of the latter (4.6×10^{-2} g, 0.14 mmol) in DMF (2 mL), ethylamine (1.1×10^{-2} mL, 0.17 mmol) and triethylamine (2.4×10^{-2} mL, 0.17 mmol) were added and the mixture was stirred at 50 °C for 7 h. The solvent was removed under reduced pressure and the residue diluted with water (2 mL) and extracted with ethyl acetate (3×1 mL). The organic layer was dried over anhydrous Na_2SO_4 and evaporated *in vacuo*. Purification by flash chromatography gave the final compound **2l** (see Scheme 1 and Table 1).

3-(3-Oxo-4,4*a*,5,6-tetrahydrobenzo[*h*]cinnolin-2(3*H*)-yl)propyl 2-amino-2-hydroxyacetate 2o. General procedure A was followed for the synthesis of 2-(3-hydroxypropyl)-4,4*a*,5,6-tetrahydrobenzo [*h*] cinnolin-3(2*H*)-one **10** from **6**. Compound **10** was obtained as a yellow oil (53% yield) upon purification by flash chromatography (eluent: dichloromethane/methanol 95 : 5). To a solution of **10** (4×10^{-2} g, 0.15 mmol) in dichloromethane (3 mL) N-Boc-Phe-OH (1.1×10^{-2} g, 0.40 mmol) and the coupling agent HATU (8.8×10^{-2} g, 0.23 mmol) were added. The solution was brought to pH = 7 with drops of *N*-methyl morpholine and it was stirred at room temperature for 24 h. The solvent was removed under reduced pressure, the residue diluted with dichloromethane (3 mL) and washed in succession with 1 N HCl (3×1 mL), saturated solution of $NaHCO_3$ (3×1 mL) and brine (2×1 mL). The solvent was dried with Na_2SO_4 and evaporated. The crude product was purified by flash chromatography (eluent: dichloromethane/ethyl acetate 85 : 15) to obtain 3-(3-oxo-4,4*a*,5,6-tetrahydrobenzo[*h*]cinnolin-2(3*H*)-yl)propyl-2-(*tert*-butoxycarbonylamino)-3-phenyl propanoate **11** as a yellow oil (33% yield). Compound **11** (3×10^{-2} g, 0.06 mmol) was dissolved in dichloromethane (3 mL) and the solution was cooled to 0 °C with an ice bath. Trifluoroacetic acid (0.05 mL, 0.71 mmol) was slowly added and the solution was stirred at room temperature for 3 h. The mixture was cooled to 0 °C, treated with a solution of 0.5 N NaOH (1 mL) and extracted with dichloromethane (3×1.5 mL). The organic layer was dried over anhydrous Na_2SO_4, filtered and evaporated *in vacuo.* Purification by flash chromatography of the crude residue afforded the final compound **2o** (see Scheme 1 and Table 1).

Synthesis of 2-(3-(2*H*-tetrazol-5-yl)propyl)-4,4*a*,5,6-tetrahydrobenzo [*h*] cinnolin-3(2*H*)-one 2p. General procedure A was followed for the synthesis of 4-(3-oxo-4,4a,5,6-tetrahydrobenzo-[*h*]cinnolin-2(3*H*)-yl)butanenitrile **12** from **6**. Compound **12** was obtained as a white solid (67% yield) upon purification by flash chromatography (eluent: dichloromethane/ethyl acetate 6 : 4). A solution of **12** (5×10^{-2} g, 0.2 mmol), sodium azide (1.2×10^{-2} g, 1.9 mmol) and zinc bromide (6.2×10^{-2} g, 0.3 mmol) in H_2O/isopropanol 2 : 1 (2 mL) was irradiated for 1 h at 170 °C in a microwave synthesizer. 6 N HCl (2 mL) was added and the mixture was extracted with ethyl acetate (3×2 mL). The organic layer was dried over anhydrous Na_2SO_4, filtered and evaporated under reduced pressure. The crude residue was purified by flash chromatography to give **2p** (see Scheme 1 and Table 1).

Synthesis of ethyl 2-(3-oxo-5,6-dihydrobenzo[*h*]cinnolin-2(3*H*)-yl)butanoate 4c. To a suspension of 5,6-dihydrobenzo[*h*]-cinnolin-3(2*H*)-one **8** (ref. 11) (5×10^{-2} g, 0.25 mmol) in toluene (1.5 mL), KOH (1.8×10^{-2} g, 0.33 mmol), TBAF·$3H_2O$ (8×10^{-3} g, 0.025 mmol) and ethyl 4-bromopropionate (0.046 mL, 0.33 mmol) were added. The mixture was heated at 50 °C for 3 h and then extracted with ethyl acetate (3×1 mL). The combined organic extracts were washed with 5% NaOH (1×2 mL) and 5% HCl (1×2 mL), dried over anhydrous Na_2SO_4, filtered and evaporated *in vacuo*. The crude product was purified by flash chromatography to obtain the final compound **4c** (see Scheme 1 and Table 1).

Synthesis of (+)-2-(2-chloroethyl)-4,4*a*,5,6-tetrahydrobenzo [*h*] cinnolin-3(2*H*)-one (+)-13. The enantiomeric separation of compound (±)-**6** was performed using a chiral semi-preparative HPLC: Chiralcel OJ (10 μm, 250 × 4.6 mm), hexane/ethanol (70 : 30), 1.0 mL min^{-1}, UV 254 nm; $t_R(1) = 2.047$ min (49.9%) $[\alpha]_D^{25}$ −561.8 (*c* 0.0055, $CHCl_3$); $t_R(2) = 2.714$ min (50.1%) $[\alpha]_D^{25}$ +572.7 (*c* 0.0055, $CHCl_3$). To a solution of (+)-**6** (5×10^{-2} mg, 0.25 mmol) in dry DMF under a nitrogen atmosphere, NaH (7.2×10^{-3} g, 0.3 mmol) and $Br(CH_2)_2Cl$ (0.025 mL, 0.3 mmol) were added. The mixture was irradiated for 15 min at 70 °C in a microwave synthesizer. The solution was evaporated under reduced pressure to remove the solvent and extracted with ethyl acetate (3 × 2 mL). The organic layer was separated, dried over anhydrous Na_2SO_4, and evaporated under reduced pressure. Upon purification by flash chromatography (eluent: petroleum ether/ethyl acetate 7 : 3), (+)-**13** was obtained as a white solid (76% yield). M.p. 127–128 °C.

Synthesis of (−)-ethyl-4-(3-oxo-4,4*a*,5,6 tetrahydrobenzo [*h*] cinnolin-2(3*H*)-yl)butanoate (−)-2c. Compound (−)-**2c** was synthesized by alkylation of (−)-**6** (5×10^{-3} g, 0.025 mmol) with $Br(CH_2)_3COOEt$ (0.004 mL, 0.03 mmol), following the same procedure as that used to obtain (+)-**13** (80% yield). Characterization of (−)-**2c** was performed using a chiral analytical HPLC: Lux cellulose-3 (3 μm, 50 × 4.6 mm), hexane/ethanol (70 : 30), 0.8 mL min^{-1}, UV 254 nm; $t_R = 1.571$ min. The result showed that the reaction occurred with less than 10% of racemization.

Biological assays

Dual-luciferase assay

Cell culture. Human colon cancer cell line (HCT-116), from American Type Culture Collection, was maintained in McCoy's 5A (Gibco/BRL). The culture medium was supplemented with 10% heat-inactivated fetal bovine serum (Gibco/BRL). Cell cultures were maintained at 37 °C under a humidified atmosphere of 5% CO_2 in an incubator.

Transient transfection and dual-luciferase assays.[17] HCT-116 cells were seeded at a density of 10×10^5 cells in a 100 mm^2 culture plate. The cells were co-transfected with pSTAT3-TA-Luc (27 μg per plate) and the internal control plasmid pRL-TK (9 μg per plate) containing the Renilla luciferase gene. All plasmids used in this experiment were purchased from Promega. The transfection was carried out using TransFectin (Bio-Rad) according to the manufacturer's protocol. After 5 h of transfection, the cells were trypsinized and seeded onto sterilized black bottom 96-well plates at a density of 1×10^4 cells per well. On the following day, cells were treated with test compounds and incubated for 24 h. Firefly and Renilla luciferase activities were measured using a dual-light reporter gene assay kit (Promega) on Wallac Victor2 (Perkin-Elmer, Inc., Wellesley, MA). The Renilla luciferase activity was determined to calibrate the transfection efficiency and cytotoxicity of chemicals. The relative STAT3 activity was calculated by dividing the firefly luciferase activity with the Renilla luciferase activity in each transfection experiment. The values of STAT3 inhibitory activity were the means of 3 experiments and the maximum deviation from the mean was less than 10%.

Alphascreen-based assay. AlphaScreen is a bead-based nonradioactive assay system for detecting biomolecular interactions in a microtiter plate format. Binding of biological partners brings donor and acceptor beads into close proximity and as a result, a fluorescent signal between 520 and 620 nm is produced. The alphaScreen-based assays[18] were performed in a final reaction volume of 25 μL of the assay buffer containing 10 mM HEPES–NaOH (pH 7.4), 50 mM NaCl, 1 mM EDTA (pH 8.0), 0.1% NP-40, and 10 ng μL^{-1} BSA in a 96-well microtiter plate at 25 °C. Phospho-Tyr (pTyr) peptide probes used in this study were 5-carboxyfluorescein (FITC)-GpYLPQTV for STAT3, FITC-GpYDKPHVL for STAT1, and FITC-PSpYVNVQN for Grb2. Firstly, 75 nM of each SH2-containing protein was incubated with the test compound for 15 min. Each protein sample was then incubated for 90 min with 50 nM of its corresponding FITC-pTyr peptide, and mixed with streptavidin coated donor beads and anti-FITC acceptor beads simultaneously before detection at 570 nm using EnVison Xcite (PerkinElmer).

Computational methods

All calculations were performed using the Gaussian09 program package,[23] at the B3LYP/6-311+G(d,p) level.[24] Theoretical values of $[\alpha]_D$ were obtained at the same level of theory specifying appropriate keywords (polar and cphf) into the Gaussian input.

X-ray crystallography

Crystals of (+)-**13** were grown by slow evaporation of a methanolic solution. Suitable single crystals were mounted on a glass fiber on a CAD4 diffractometer with graphite monochromated MoKα radiation (λ 0.71073 Å). The cell parameters were determined and refined by least-squares fit of 25 high angle reflections. The structure was resolved by direct methods using Sir-92 (ref. 25) and completed by iterative cycles of full-matrix least squares refinement on F_o^2 and Δ*F* synthesis using the SHELXL-97 program (WinGX suite).[26] All non-H-atoms were refined anisotropically. The H-atoms of (+)-**13** were detected in the Fourier map. Geometrical calculations were carried out with the program PARST.[27] The absolute configuration of (+)-**13** was unambiguously determined by refining the Flack parameter (−0.04(15)), exploiting the anomalous scattering effects of chlorine.[28]‡ Crystal data for (+)-**13**: $C_{14}\,H_{15}\,N_2\,O_1\,Cl_1$, $M_r = 262.73$ g mol^{-1}, orthorhombic, space group $P2_12_12_1$, $a = 7.929(4)$ Å, $b = 12.530(4)$ Å, $c = 12.977(8)$ Å, $V = 1289.3(8)$ $Å^3$, $Z = 4$, $D_{calc} = 1.354$ mg m^{-3}, F(000) = 552, $R = 0.041$ (reflections collected/unique = 1825/1806), w*R*2 = 0.095, $T = 293(2)$ K, GOF = 0.948. The reflections were collected in the range of $2.26° \leq \theta \leq 24.97°$ (limiting indices = $-1 \leq h \leq 9$, $-1 \leq k \leq 14$, $-1 \leq l \leq 15$) employing a 0.9 × 0.4 × 0.3 mm crystal. The residual positive and negative electron densities in the final map were 0.142 and –0.244 e $Å^{-3}$, respectively.

‡ The supplementary crystallographic data have been deposited at the Cambridge Crystallographic Data Centre: CCDC deposition number 906024. These data can be obtained free of charge *via* www.ccdc.cam.ac.uk/conts/retrieving.html (or from CCDC, 12 Union Road, Cambridge CB2 1EZ, UK; fax: +44 1223 336033; deposit@ccdc.cam.ac.uk).

Acknowledgements

This study was supported by funds from PRIN 2010–2011. The authors also thank the Universities of Milan and Pavia (PUR and FAR grants, respectively), the National Research Foundation of Korea (NRF-2011-0015768), and Fondazione Confalonieri (Fellowship 2012) for the financial support.

References

1 L. Costantino and D. Barlocco, *Curr. Med. Chem.*, 2008, **15**(9), 834–843.
2 B. B. Agganwal, A. B. Kunnumakkara, K. B. Harikumar, S. R. Gupta, C. K. Tharakan, S. Dey and B. Sung, *Ann. N. Y. Acad. Sci.*, 2009, **1171**, 59–76.
3 T. Bowman, R. Garcia, J. Turkson and R. Jove, *Oncogene*, 2000, **19**(21), 2474–2488.
4 R. Buettner, R. B. Mora and R. Jove, *Clin. Cancer Res.*, 2002, **8**(4), 945–954.
5 Y. Nefedova, M. Huang, S. Kusmartsev, R. Bhattacharya, P. Cheng, R. Salup, R. Jove and D. Gabrilovich, *J. Immunol.*, 2004, **172**(1), 464–474.
6 T. Bowman, M. A. Broome, D. Sinibaldi, W. Wharton, W. J. Pledger, J. M. Sedivy, R. Irby, T. Yeatman, S. A. Courtneidge and R. Jove, *Proc. Natl. Acad. Sci. U. S. A.*, 2001, **98**(13), 7319–7324.
7 J. Turkson, D. Ryan, J. S. Kim, Y. Zhang, Z. Chen, E. Haura, A. Laudano, S. Sebti, A. D. Hamilton and R. Jove, *J. Biol. Chem.*, 2001, **276**(48), 45443–45455.
8 D. Masciocchi, A. Gelain, S. Villa, F. Meneghetti and D. Barlocco, *Future Med. Chem.*, 2011, **3**(5), 367–397.
9 D. Bikash, X. Shili and N. Nouri, *J. Med. Chem.*, 2012, **55**(15), 6645–6668.
10 K. Matsuno, Y. Masuda, Y. Uehara, H. Sato, A. Muroya, O. Takahashi, T. Yokotagawa, T. Furuya, T. Okawara, M. Otsuka, N. Ogo, T. Ashizawa, C. Oshita, S. Tai, H. Ishii, Y. Akiyama and A. Asai, *ACS Med. Chem. Lett.*, 2010, **1**, 371–375.
11 H. Chen, Z. Yang, C. Ding, L. Chu, Y. Zhang, K. Terry, H. Liu, Q. Shen and J. Zhou, *Eur. J. Med. Chem.*, 2013, **62**, 498–507.
12 D.-S. Shin, H.-N. Kim, K. D. Shin, Y. J. Yoon, S.-J. Kim, D. C. Han and B.-M. Kwon, *Cancer Res.*, 2009, **69**, 193–202.
13 D.-S. Shin, D. Masciocchi, A. Gelain, S. Villa, D. Barlocco, F. Meneghetti, A. Pedretti, Y.-M. Han, D. C. Han, M. Y. Han, B.-M. Kwon, L. Legnani and L. Toma, *Med. Chem. Commun.*, 2010, **1**(2), 156–164.
14 D. Masciocchi, S. Villa, F. Meneghetti, A. Pedretti, D. Barlocco, L. Legnani, L. Toma, B.-M. Kwon, S. Nakano, A. Asai and A. Gelain, *Med. Chem. Commun.*, 2012, **3**, 592–599.
15 L. Costantino, G. Rastelli, K. Vescovili, G. Cignarella, P. Vianello, A. Del Corso, M. Cappiello, U. Mura and D. Barlocco, *J. Med. Chem.*, 1996, **39**, 4396–4405.
16 A. D. Khanolkar, D. Lu, P. Fan, X. Tian and A. Makriyannis, *Bioorg. Med. Chem. Lett.*, 1999, **9**(15), 2119–2124.
17 B. A. Sherf, S. L. Navarro, R. R. Hannah and K. V. Wood, *Promega Notes Magazine*, 1996, vol. 57, pp. 2–8.
18 Y. Uehara, M. Mochizuki, K. Matsuno, T. Haino and A. Asai, *Biochem. Biophys. Res. Commun.*, 2009, **380**, 627–631.
19 L. Toma, G. Cignarella, D. Barlocco and F. Ronchetti, *J. Med. Chem.*, 1990, **33**, 1591–1594.
20 (*a*) P. J. Stephens, F. J. Devlin, J. R. Cheeseman, M. J. Frisch and C. Rosini, *Org. Lett.*, 2002, **4**, 4595–4598; (*b*) B. Mennucci, J. Tomasi, R. Cammi, J. R. Cheeseman, M. J. Frisch, F. J. Devlin, S. Gabriel and P. J. Stephens, *J. Phys. Chem. A*, 2002, **106**, 6102–6113; (*c*) E. Giorgio, M. Roje, K. Tanaka, Z. Hamersak, V. Sunjic, K. Nakanishi, C. Rosini and N. Berova, *J. Org. Chem.*, 2005, **70**, 6557–6563; (*d*) A. C. Petrovic, J. He, P. L. Polavarapu, L. S. Xiao and D. W. Armstrong, *Org. Biomol. Chem.*, 2005, **3**, 1977–1981; (*e*) M. Zappala, G. Postorino, N. Micale, S. Caccamese, N. Parrinello, G. Grazioso, G. Roda, F. S. Menniti, G. De Sarro and S. Grasso, *J. Med. Chem.*, 2006, **49**, 575–581.
21 C. K. Johnson, *ORTEP 11, Report ORNL-5138*, OakRidge National Laboratory, TN, 1976.
22 D. Cremer and J. A. Pople, *J. Am. Chem. Soc.*, 1975, **97**, 1354–1358.
23 M. J. Frisch, G. W. Trucks, H. B. Schlegel, G. E. Scuseria, M. A. Robb, J. R. Cheeseman, G. Scalmani, V. Barone, B. Mennucci, G. A. Petersson, H. Nakatsuji, M. Caricato, X. Li, H. P. Hratchian, A. F. Izmaylov, J. Bloino, G. Zheng, J. L. Sonnenberg, M. Hada, M. Ehara, K. Toyota, R. Fukuda, J. Hasegawa, M. Ishida, T. Nakajima, Y. Honda, O. Kitao, H. Nakai, T. Vreven, J. A. Montgomery, Jr, J. E. Peralta, F. Ogliaro, M. Bearpark, J. J. Heyd, E. Brothers, K. N. Kudin, V. N. Staroverov, R. Kobayashi, J. Normand, K. Raghavachari, A. Rendell, J. C. Burant, S. S. Iyengar, J. Tomasi, M. Cossi, N. Rega, J. M. Millam, M. Klene, J. E. Knox, J. B. Cross, V. Bakken, C. Adamo, J. Jaramillo, R. Gomperts, R. E. Stratmann, O. Yazyev, A. J. Austin, R. Cammi, C. Pomelli, J. W. Ochterski, R. L. Martin, K. Morokuma, V. G. Zakrzewski, G. A. Voth, P. Salvador, J. J. Dannenberg, S. Dapprich, A. D. Daniels, Ö. Farkas, J. B. Foresman, J. V. Ortiz, J. Cioslowski and D. J. Fox, *Gaussian 09, Revision A.02*, Gaussian, Inc., Wallingford CT, 2009.
24 (*a*) C. Lee, W. Yang and R. G. Parr, *Phys. Rev. B: Condens. Matter Mater. Phys.*, 1988, **37**, 785–789; (*b*) A. D. Becke, *J. Chem. Phys.*, 1993, **98**, 5648–5652.
25 A. Altomare, M. C. Burla, M. Camalli, G. L. Cascarano, C. Giacovazzo, A. Guagliardi, A. G. G. Moliterni, G. Polidori and R. R. Spagna, *J. Appl. Crystallogr.*, 1999, **32**, 115–119.
26 L. J. Farrugia, *J. Appl. Crystallogr.*, 1999, **32**, 837.
27 M. J. Nardelli, *J. Appl. Crystallogr.*, 1995, **28**, 659.
28 H. D. Flack, *Acta Crystallogr., Sect. A: Found. Crystallogr.*, 1983, **A39**, 876–881.

